# Program and algorithmic complex for synthesis of dynamic photo analysis of the aging degree of rubbers

D.V. Sklyarevskiy[a], A.A. Khvostov[b], V.I. Ryazhkih[c], S.G. Tikhomirov[a], I.A. Khaustov[a]

[a] *Voronezh State University of Engineering Technologies, 394036, Revolution Av., 19, Voronezh, Russia*
[b] *MERC "Zhukovsky – Gagarin Air Force Academy", 394064, Staryh Bolshevikov St., 54 "A", Voronezh, Russia*
[c] *Voronezh State Technical University, 394026, Moscow Av., 14, Voronezh, Russia*

**Abstract**

The article describes program and algorithmic complex for synthesis of computer vision. This method operates as part of an automated control system for climate testing and it designs to analyze the aging of rubber products according to their visual indices. In this article the structural scheme of the system has been given. In addition, modified methods have been described. They compare the coordinates of a series of photographs, eliminate noise in the image being processed, and convert the output data of the computer vision algorithms into aging characteristics of rubbers. A brief description of the software of the operator-researcher has been presented.

*Keywords:* computer vision; rubber; crack; climatic tests; aging

## 1. Introduction

The influence of climatic factors (such as oxygen and ozone, light, temperature, humidity) worsens the physical and mechanical properties, and as a consequence, destroys the rubber products (RP) because of the aging process.

Along with various mechanical tests to develop new formulations of RPs, as well as quality control of existing products, a number of tests of product samples on the resistance to deterioration are carried out under the influence of aging factors [1]. Climatic chambers (CC) are used to control the climatic testing processes of the RP. They allow to simulate the effects of aggressive climatic factors (operating conditions on identical test) the test samples of the RP.

The degree of destruction of RP is assessed using an analysis of photographs of the product obtained with the help of optical means.

Methods of machine vision in the context of crack analysis have been successfully applied to assess the degree of deterioration of road surfaces [2], destruction of reinforced concrete structures [3], damage to metal structures [4], etc. However, an automatic analysis of the degree and nature of the destruction of RP with the use of computer vision methods has not found wide application in the QC testing process in view of the absence of algorithms for processing and visualizing information specific for aging processes of RP.

Thus, development of a program and algorithmic complex for synthesis of dynamic photo analysis of the aging degree of rubbers for the automated control system for climatic testing of RP with the use of computer vision methods is an actual scientific and technical task.

## 2. The object of the study

### *2.1 Experiments*

A number of experimental studies had been carried out to artificially age a number of product samples in order to obtain the initial data for testing the developed image processing algorithms that provide visual information on the degree and nature of the destruction of the RP. Samples had been made from various rubbers.

During the experiments series of images of vulcanizate samples with different filler contents in real time was obtained (table 1). The samples were exposed to unfavourable weather conditions (sunlight, humidity, atmospheric pollution, such as ozone and nitrogen oxides), which were exerted a direct destructive effect on them.

The difference between the samples depends on the antioxidants. This allows us to analyze the images for different patterns of sample destruction.

### *2.2 Program and algorithmic complex*

The developed program and algorithmic complex is represented by a subsystem that is part of a larger subsystem of dynamic photo analysis of the automated control system for climatic of aging RP samples located in a climatic chamber (see fig. 1).

**Table 1.** Formulations of RP samples [Mass units]

| Composition | 1 | 2 | 3 |
|---|---|---|---|
| Natural rubber | 50.0 | 50.0 | 50.0 |
| Rubber SKS-30 ARK | 50.0 | 50.0 | 50.0 |
| Sulfur | 2.0 | 2.0 | 2.0 |
| Altaks | 3.0 | 3.0 | 3.0 |
| Zinc Oxide | 5.0 | 5.0 | 5.0 |
| Stearic acid | 2.0 | 2.0 | 2.0 |
| Chalk | 10.0 | 10.0 | - |
| White soot BS-120 | - | - | 15.0 |
| Tire regenerate RSHT | - | 15.0 | - |
| Result: | 122.0 | 137.0 | 127.0 |

The aging process of rubbers differs in their physical properties for each formulation in particular. This requires the modification of existing algorithms of machine vision with new stages and indicators that could allow to assess the degree and nature of aging RP in dynamics.

In the future, this allows us to proceed to the development of a program complex, which converts the output data of typical and modified computer vision algorithms into quantitative estimates of the aging degree of RPs, convenient for interpretation the decision-making.

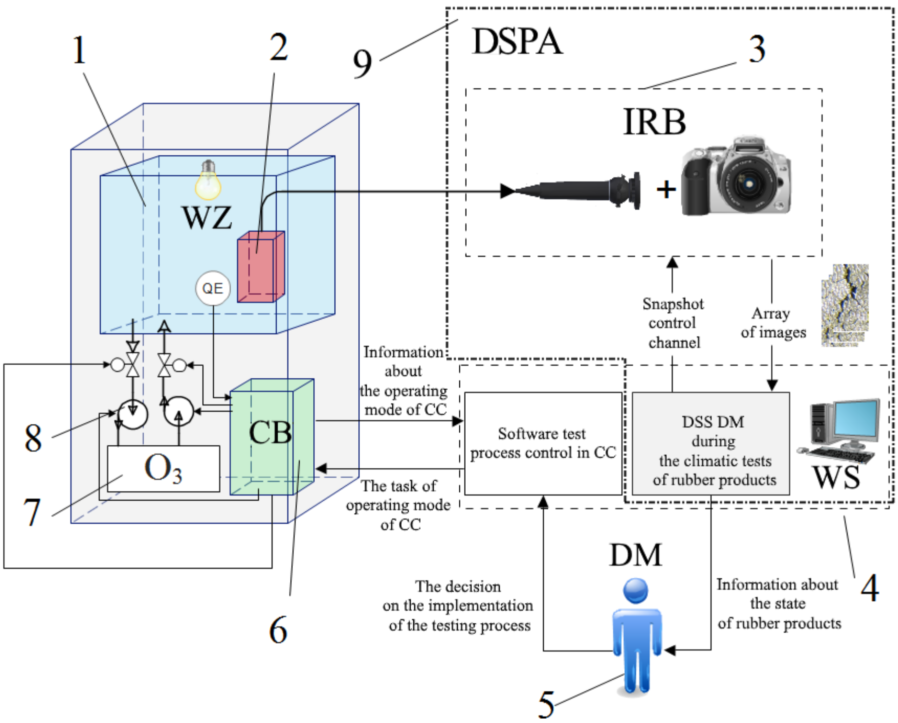


**Fig. 1.** Function structure diagram of automated system for control climating testing of RP on an example of the ozone test chambers: 1 - working zone (WZ) of CC with the light source; 2 - RP sample; 3 - image registration block (IRB) presented as a digital camera interfaced with an industrial fiberscope; 4 - workstation; 5 - a person who makes a decision on the course of the testing process (Decision Maker DM); 6 - control block (CB) of CC; 7 - ozone station; 8 - ozone concentration control loop in the work zone of CC; 9 - dynamical subsystem of photo-analysis (DSPA) of RP's of aging degree.

The figure 2 shows the structure blocks of interrelated program blocks.

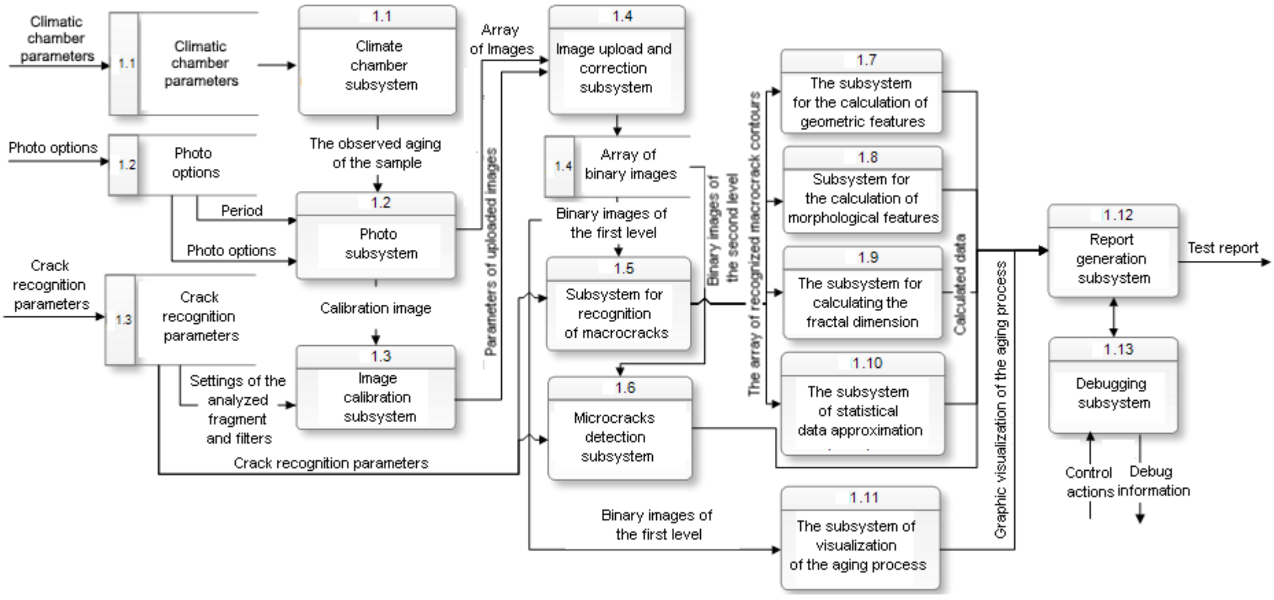


**Fig. 2.** The interaction of the subsystems of the dynamic photoneasurement of aging rubbers.

## 3. Methods

### *3.1. Algorithms*

Algorithms and techniques have been developed to ensure a reliable interpretation of the recognized damage and the subsequent implementation of the program and algorithmic complex, such as:

– correction algorithm of coordinates where the analyzed fragment is attached to the marking of the working section of the sample in series of images, which is characterized use of an additional cluster estimation after the comparison of the key points revealed by the algorithm "Scale-Invariant Feature Transform" ("SIFT") [5]. This makes it possible to reduce the error probability when the coordinates compares the analyzed image fragment before and after the deformations of the sample (occur during testing from 30% to 8%). The results of comparison of new algorithm with the RANSAC algorithm [5] are shown in table 2:

**Table 2.** Tests results of algorithm of the correction area of interest

| Sample No | The area, mm | Percent Difference, % | |
|---|---|---|---|
| | | SIFT + RANSAC | SIFT + cluster correction |
| 1 | 8,8 × 5,6 | 35 | 8 |
| 2 | 9 × 7,6 | 31 | 5 |
| 3 | 9,0 × 8,3 | 32 | 5 |
| Average: | | 32,7 | 6 |

– Image filtering and improving techniques of sample surface of the RP includes the application of the Single Scale Retinex ("SSR") elimination algorithm and the combined use of a bilateral filter with an adaptive threshold filter [6] in order to eliminate image defects not related to defects such as a crack (for example, water stains due to surface wetting of the RP sample);

– The technique of obtaining the dynamic characteristics of aging RP *Ps* (1), and estimating the fractal dimension of the cracking surface. It allows to establish the degree of crack nucleation and growth.

$$Ps = \left\{ Ps_{k,z}, \quad k = \overline{1,K}, z = \overline{1,Z} \right\}, \tag{1}$$

where *K* is a number of cracks; *Z* is a number of calculated morphological characteristics.

Each element of the set $Ps_{k,z}$ contains subset of the crack's attribute (2):

$$Ps_{k,z} = \left\{ S, P, W_{avg}, W_{max}, L_{max}, L_{full}, \varphi, C, Db, Nb, Dim_M \right\}, \tag{2}$$

where $S$ is an area of crack [mm$^2$]; $P$ is a perimeter of crack [mm]; $W_{avg}$ is an average opening width [mm]; $W_{max}$ is a maximum opening width [mm]; $L_{max}$ is a maximum length of the longest segment [mm]; $L_{full}$ is a sum of lengths of all the segments [mm]; $\varphi$ is a crack's angle [°];$C$ is a degree of the crack's curvature relative to a straight line; $Db$ is a crack's branching index; $Nb$ is a number of segments; $Dim_M$ is a Minkowski fractal dimension.

– method for assessing the degree merging of cracking [7]. The quantitative attribute was proposed. It characterizes the intensity of the fusion process (in fractions of the total). This indicator allows us to identify areas where destruction will occur in the near future (3):

$$J = \begin{cases} 1 - \dfrac{N_a}{N_b}, \; if \;\; N_b > 0, \\ 0, \; else, \end{cases} \qquad (3)$$

where $N_b$ и $N_a$ cracks before and after merger, respectively.

– algorithm for calculating the parameters of a grid of microcracks on the surface of RP sample using Hough transform [6, 8], which allows to determine the average width of grid cells and the average distance between cell centers.

– modified wave algorithm [9], which allows to perform the calculation of the maximum number of geometric and morphological crack's parameters (average and maximum opening width, length of the longest segment of the crack, the total length of the cracks, the number of branches of the crack), and to produce the segmentation of cracks that takes an opportunity to present a crack as a connected graph. Here we can determine the crack's branching index (4):

$$Db = \frac{\sum_{j=1}^{Nb} L_{b\,j}}{L_{max}} - 1, \qquad (4)$$

where $L_{b\,j}$ is the length of the $j$-th branch of the crack, $L_{max}$ is the length of the longest segment of the crack (the skeleton).

Cracks branching index $Db$ are shown in fig. 3.

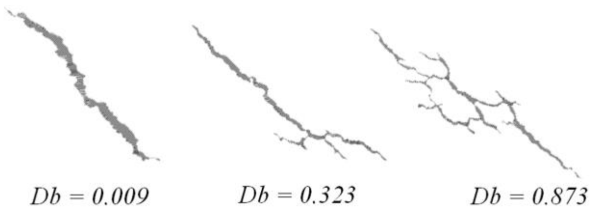


**Fig. 3.** Cracks branching index.

– a visualization method of the destruction process based on the imposing of binary images. This method allows to visualize the centers of crack's propagation.

*3.2. Software realization*

Program and algorithmic complex is a DSS which was realized in the Qt Creator 3.2.1 using C++ and computer vision library OpenCV [10].

DSS has a set of functions for calculation of the RP's fracture (area, length, width, angle, fractal dimension of defects, etc.). It contains a statistical analysis of defects, a detailed analysis of each defect, the analysis of surface crack's grid, which may be useful to DM. The main form of the program is shown in fig. 4. The form of processing statistical data is shown in fig. 5.

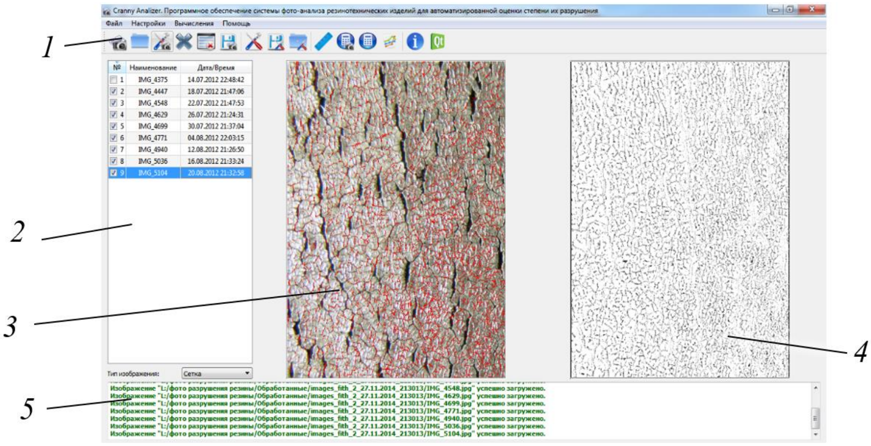

**Fig. 4.** Main form of the program: 1 is a toolbar; 2 is a list of loaded images; 3 is a panel which shows the current image with the detected microcracks; 4 is a panel which shows the binary image with the detected defects; 5 is an information console.

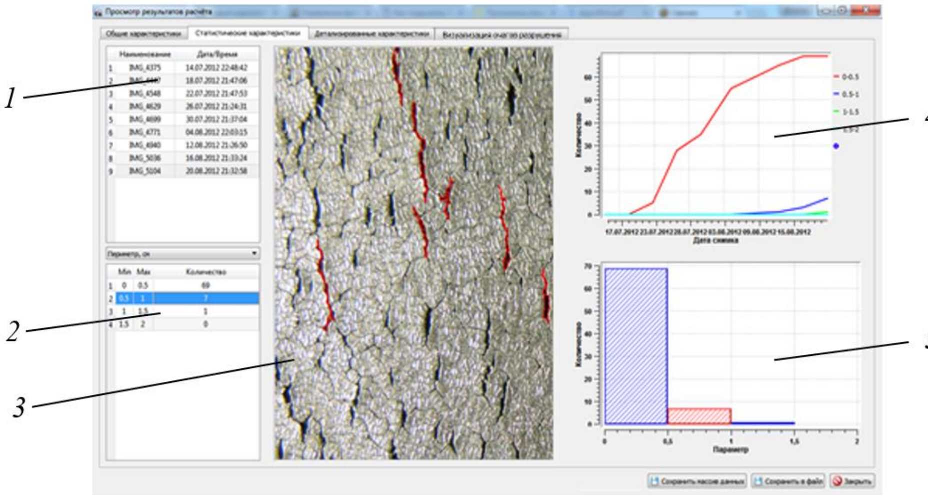

**Fig. 5.** Statistic view tab characteristics of destruction in viewing analysis results: 1 is a list of analyzed images; 2 is a list interval parameters; 3 is a component of mapping the cracks occuring in selected interval; 4 diagram with changing the parameters entering certain interval of time 5 is a histogram of the distribution of parameters for the selected image.

**Table 3.** Fields description of the program output

| No | Field name | Description |
|---|---|---|
| 1 | ID | Crack's identifier |
| 2 | Day_num | Number of days performing photographing |
| 3 | x | Coordinate of the center of crack along the horizontal axis, mm |
| 4 | y | Coordinate of the center of crack along the veRPcal axis, mm |
| 5 | S | Area of crack, mm$^2$ |
| 6 | P | Perimeter of crack, mm |
| 7 | Wavg | Average opening width, mm |
| 8 | Wmax | Maximum opening width, mm |
| 9 | Lfull | Full length of crack, mm |
| 10 | Lmax | Length of the longest segment of crack, mm |
| 11 | Angle | Crack's angle,$^\circ$ |
| 12 | FrDim | The fractal dimension of crack |
| 13 | CombCount | Number of merge of crack |
| 14 | BranchCount | Number of branches of crack |
| 15 | Curvature | Curvature index of crack |
| 16 | BranchDegree | Branching index of crack |

Furthermore the DSS has a flexible configuration for various test conditions and includes two groups of adjustable parameters, namely, pre-imaging (coordinates of analyzed fragment, the rotation angle of the image, the parameters of «SSR» filter, a two-level adaptive threshold and bilateral filters etc.) and cracks detection (minimum distance of cracks merging, the minimum allowable length of the crack's branching, the parameters for calculation of the Minkowski fractal dimension, the parameters of recognition algorithm for the grid of surface microcracks).

## 4. Results and Discussion

The developed software allows to export the table of characteristics of each image and each crack. The table 3 of characteristics of detected cracks has the form.

Analysis of dynamic crack with a difference of 3 days are presented in fig. 6 (without merging) and fig. 7 (with merging).


a) b)

**Fig. 6.** An example of dynamic crack without merging with a difference of 3 days.

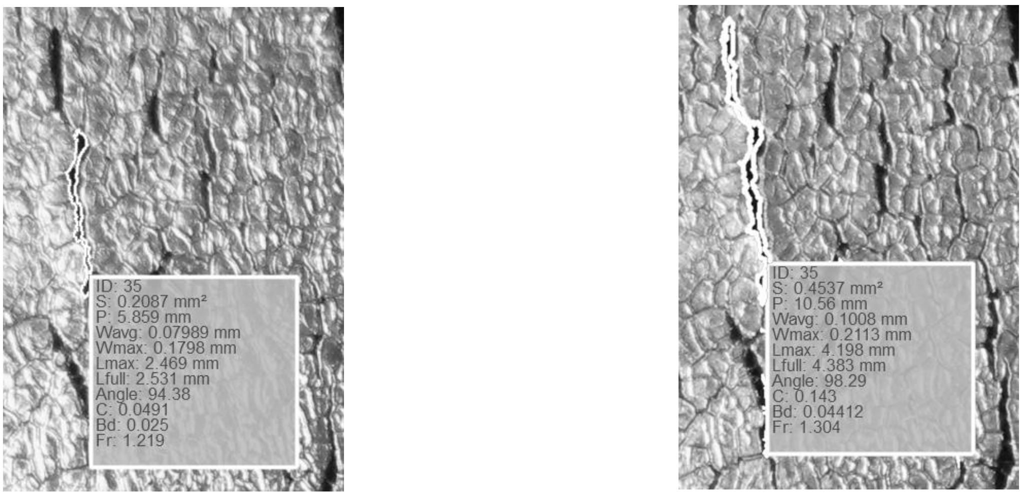


a) b)

**Fig. 7.** An example of dynamic crack with merging with a difference of 3 days.

The dynamical characteristics of the aging RP's can be plotted using the obtained data in the program itself and through external software (Excel, Matlab, Mathcad, etc.) Examples of dynamical characteristics for three samples of RP made with the different rubber composition are shown in fig. 8.

Also the developed software allows to determine the centers and the direction of crack's propagation (see fig. 9).

In this way the presented software reduces the load on the DM and decreases the subjective assessment of the degree and nature of climatic aging of RP. Also there is a possibility for accumulation of experimental data for further processing and identification of new data (identification of centers of crack propagation, evaluation of active merging formation process, evaluation of statistical indexes of the aging process).

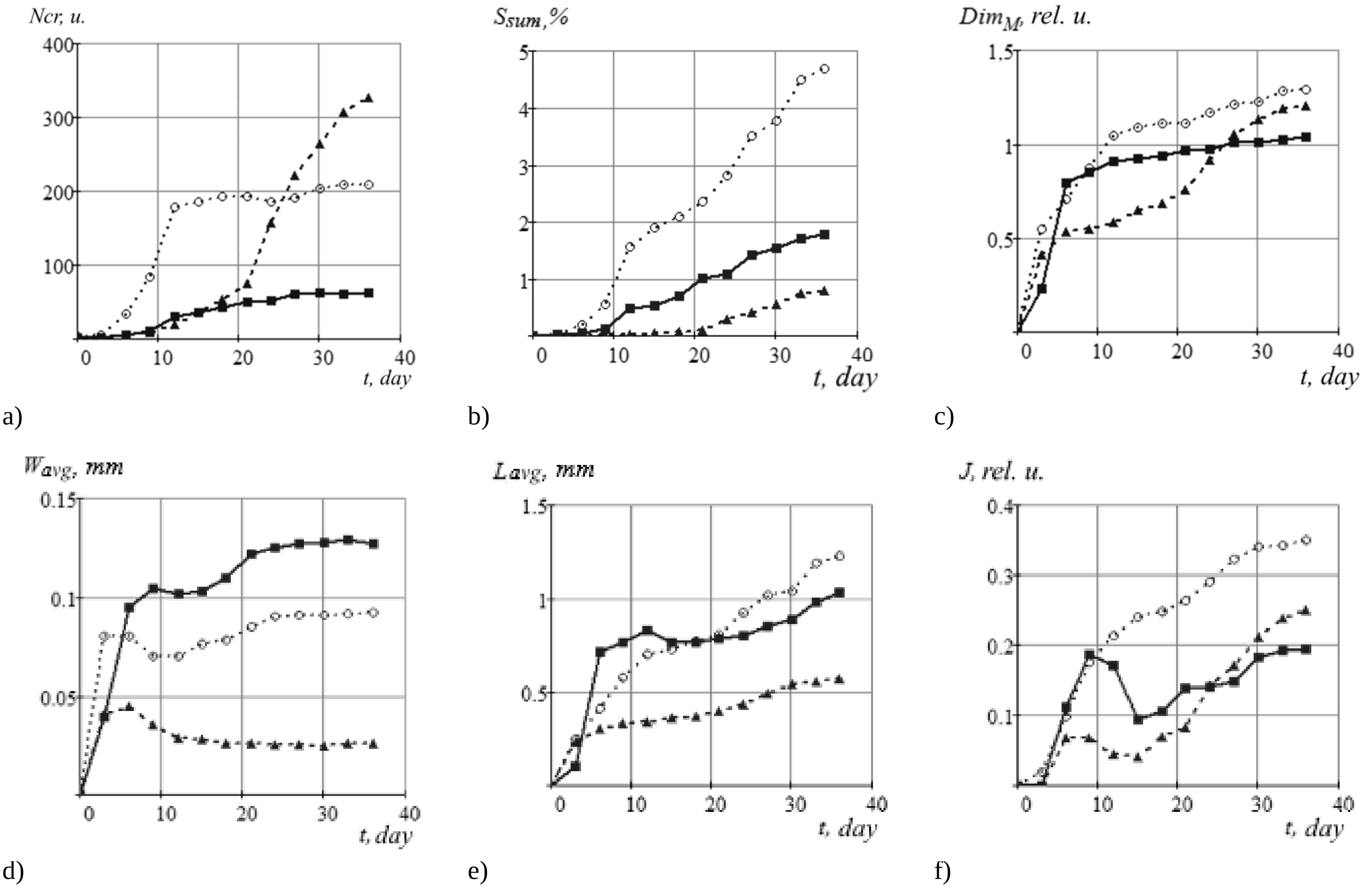


**Fig. 8.** Dynamical chracteristics of aging: panel a – number of cracks, panel b – total area as a percentage of the total area of the sample's surface, panel c – Minkowski fractal dimension, panel d – average crack width, panel e – average crack length, panel f – cracks merger index. Here ○⊙○ is a sample 1; ■■■ is a sample 2; ▲▲▲ is a sample 3.

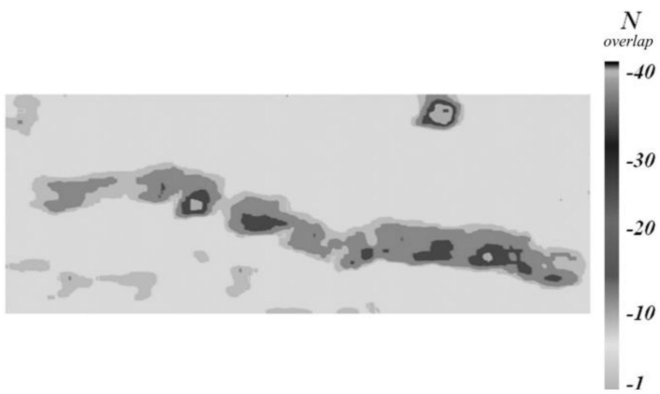


**Fig. 9.** Visualization of the destruction centers, where *Noverlap* is a number of matching pixels at each point when the binary images obtained by a series of photographs are superimposed.

## 5. Conclusions

The proposed method allowed additionally to take into account their visual characteristics in the framework of the automated control system for climatic testing of RP. The developed toolkit is focused on passive quality monitoring of RPs and is made it possible to carry out an active experiment in the course of research, changing the parameters of climatic tests and identifying a system link between the a RP ficially created conditions and the aging degree of RP. In addition, the creation of conjugated database and mathematical models formalize the dynamics of changes in the quality of RP during the climate test and provide additional information for making a decision on the advisability of modification of the RP formulations, as well as the management of the relevant technological processes.


## Acknowledgements

The authors express their gratitude to the members of the "Chemistry and Chemical Technology of organic compounds and polymers processing" department of "Voronezh State University of Engineering Technology" Prof. Karmanova O.V. and Dr.

Molchanov V.I. for their valuable advice, training and providing of experimental samples of rubber as well as Dr. Rebrikov D.I. for assistance in carrying out the experimental research.

## References

[1] ISO 1431-1:2012 Rubber, vulcanized or thermoplastic – Resistance to ozone cracking. Part 1: Static and dynamic strain testing. 2012. 17 p.
[2] Li, L. Automatic pavement crack recognition based on BP neural network / L. Li, L. Sun, G. Ning, S. Tan // Promet. Traffic&Transportation. 2014. Vol. 26, No. 1. P. 11-22.
[3] Zhang, W. Automatic Crack Detection and Classification Method for Subway Tunnel Safety Monitoring / W. Zhang, Z. Zhang, D. Qi, Y. Liu // Sensors. 2014. No. 14. P. 19308-19328. – doi:10.3390/s141019307.
[4] Broberg, P. Detection of Surface Cracks in Welds using Active Thermography / P. Broberg, A. Runnemalm // 18th World Conference on Nondestructive Testing, Durban, South Africa. 2012. P. 16-20.
[5] Lowe, D. Distinctive Image Features from Scale-Invariant Keypoints / D. Lowe // In International Journal of Computer Vision. 2004. Vol. 60. P. 91-110.
[6] Shapiro, L.G. Computer Vision / L.G. Shapiro, G.C. Stockman. Moscow: Binom, 2006. 752 p.
[7] Khvostov, A.A. Methods of assessing the degree of destruction of rubber products using computer vision algorithms / A.A. Khvostov, D.V. Sklyarevskiy, A.A. Nikitchenko // Proceedings of the Voronezh State University of Engineering Technologies. 2015. N 2 (64). P. 72-76.
[8] Khvostov, A.A. Application of machine vision algorithms to detect grid hairline cracks on the surface of rubber products / A.A. Khvostov, S.G. Tikhomirov, D.I. Rebrikov, D.V. Sklyarevskiy // Control Systems and Information Technology. 2015. N 3 (61). P. 93-96.
[9] Sklyarevskiy, D.V. The formalization of morphological signs of surface cracks of rubber products using the wave algorithm / D.V. Sklyarevskiy, A.A. Khvostov, S.G. Tikhomirov, A.A. Nikitchenko // Proceedings of the Voronezh State University. Series: "System Analysis and Information Technologies". 2016. N 1. P. 65-71.
[10] OpenCV 2.4.11.0 documentation [Electronic resource]. – Access mode: http://docs.opencv.org/ (05.02.2015).